GEOCHEMISTRY: MAJOR OXIDES

It may be suspected that volcanic rocks of Carboniferous-Triassic age would be sufficiently altered to make petrochemical studies unrewarding. Perhaps this was the reason that the Panjal Traps did not attract much attention of geochemists. Wadia (1934) observed that epidotization, chloritization, and silicification is common in these rocks. However, a careful search usually reveals fairly clean unaltered material. Olivine, which is an easy prey to alteration processes, is absent from the mode of these rocks, thus reducing the chances of easy alteration. On a scale involving the present area of investigation the Panjal Traps appear to be heterogeneous in the nature and extent of alteration. Some crystals in the rocks have undergone alteration to epidotes, chlorites, and tremolite-actinolite but have retained the primary igeneous characters.

The recognition of specific magmatic character can best be approached by reconstruction of bulk chemical composition by deriving an average composition from analysis of many samples of a single lava flow (Smith, 1968; Vallence, 1969, 1974) or by consideration of relic primary phase chemistry, in particular that of pyroxenes (Vallence, 1969, 1974). The former approach is essentially preferred in the present study because of the absence of pyroxene phenocrysts in the Panjal Traps.

TABLE II

Average chemical composition of the Panjal Traps compared with the average chemical composition of Karroo basalts (Anhydrous basis).

	Panjal Traps	Karroo basalts
SiO_2	51.12	52.7
TiO_2	1.75	1.16
Al_2O_3	14.36	15.4
Fe_2O_3	1.84	1.38
FeO	8.95	9.35
MgO	5.59	6.60
CaO	9.87	9.96
Na_2O	3.15	2.22
K_2O	1.14	0.87
MnO	0.11	0.22
P_2O_5	0.17	0.16

Data source:

Panjal Traps: Present study

Karroo basalts: Adopted from Cox et al. (1967, Table 3).

In Table II average chemical composition of the Panjal Traps is compared with the average chemical composition of the Karroo basalts. The selection of the Karroo basalts for comparison with the Panjal Traps was mainly preferred because of the much similarity in the petrology of the two lava formations besides, the Karroo Volcanic Province being one of the few well studied basalt formations of the world. The close similarity in chemical composition, as seen from Table II, indicates that the alteration in the Panjal Traps has largely been isochemical excluding the concentration of more mobile alkali elements. This may further be tested on ACN face of ACFN tetrahedron of Smith (1968). Jolly and Smith (1972) found Keweenawan basalts to plot in three regions on ACN face of ACFN diagram. These three regions, unaltered basalts (I), basalts containing albitized feldspar (II), and basalts with chlorite, epidote, prehnite, and laumonite (III), represent the three types of basalts that exist in the Keweenawan lavas. Figure 6 shows that the Panjal Traps almost invariably plot in the unaltered basalt region (I) on this diagram. This may indicate that these rocks are compositionally unaltered. However, some of the plots occupy the common region of unaltered basalts (I) and albite rich basalts (II). These plots may represent the samples that were highly affected by alkali metasomatism. This inference is consistent with microscopic observations of these samples; secondary albite and

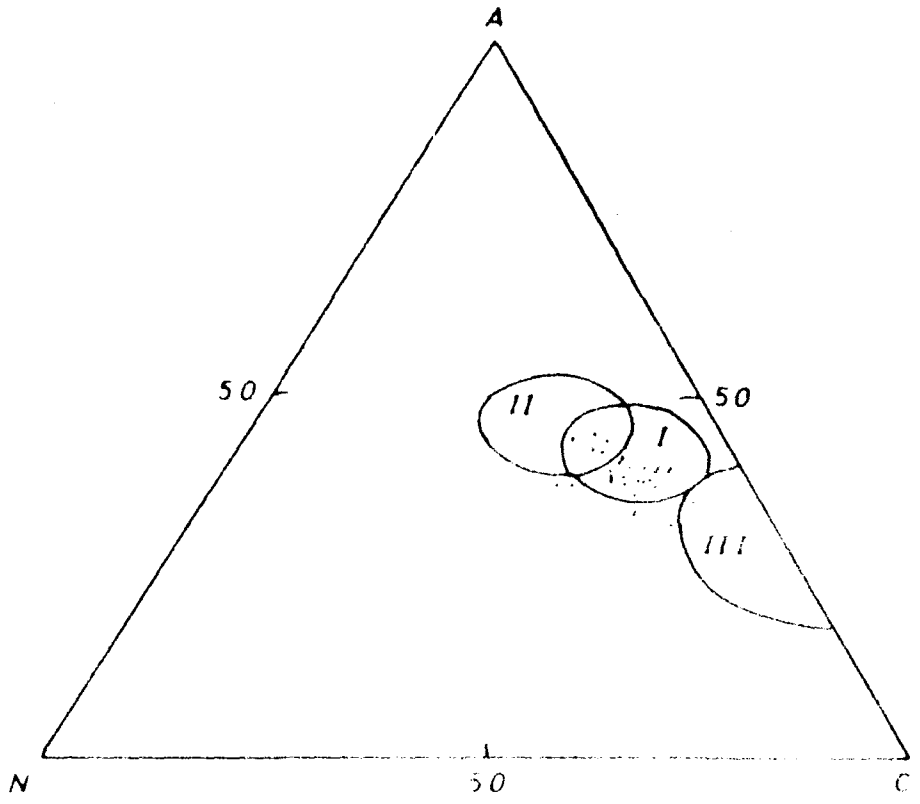

Figure 6. Plots of the Panjal Traps on ACN face of ACFN tetrahedron. Subdivisions, from Jolly and Smith (1972), are (I) Unaltered basalts, (II) basalts containing albitized feldspar; (III) metadomians; chlorite; pumpellyite; epeidote, prehnite, laumonite. A = $Al_2O_3 - K_2O$; C = CaO, N = Na_2O (All in molecular proportions).

biotite are found to exist in large amounts in these rocks. Thus, the largely isochemical nature of the alteration seems responsible for retaining still recognizable magmatic texture in these rocks.

Coombé (1963) suggested that chemical analyses of various basalts can most satisfactorily be compared with each other (especially on normative plots) if their contents of Fe_2O_3 are reduced somewhat to allow for the post-extrusion oxidation of lava. The scale of reduction proposed by Coombs (1963) is as follows:

1. If total alkali is less than 4% in the rock then Fe_2O_3 should be taken as 1.50% for normative calculations.
2. If total alkali is 4-7%, then Fe_2O_3 should be taken as 2.00%, and
3. If total alkali is 7-10%, then Fe_2O_3 should be taken as 2.5%.

Chayes (1966) considered basalt with Fe_2O_3/FeO ratio greater than 0.6 as altered. Irvine and Barager (1971) placed an upper limit of Fe_2O_3 for normative calculations according to the following equation:

$$\text{Percent } Fe_2O_3 = \text{Percent } TiO_2 + 1.5$$

This equation is based on the observation that TiO_2 and Fe_2O_3

TABLE III

Chemical and normative composition of the Panjal Traps

Flow No.	1	2	3	4	5	6	7	8	9	10	11	12	13	14	15	16
SiO_2	49.76	50.85	51.68	51.31	51.09	50.88	49.38	49.18	48.19	49.67	50.61	52.53	52.92	50.41	50.97	52.22
TiO_2	1.64	1.37	1.35	2.09	1.96	1.94	1.44	2.02	2.15	2.11	1.99	1.88	2.21	2.13	2.12	2.15
Al_2O_3	14.71	14.29	14.02	14.48	14.16	14.20	14.20	14.37	13.33	13.19	14.72	14.66	14.53	13.18	14.89	14.46
Fe_2O_3	2.15	2.08	2.04	2.15	2.08	2.18	1.94	1.81	1.36	0.85	1.12	1.48	1.82	1.53	1.30	1.20
FeO	8.97	8.15	9.60	8.78	9.05	9.65	9.94	9.65	9.32	8.17	8.83	8.96	8.64	9.45	9.69	8.61
MgO	5.44	5.97	5.73	5.60	6.67	5.48	6.85	6.96	6.84	5.56	4.95	5.21	4.98	6.07	4.67	5.02
CaO	13.06	11.99	10.30	10.49	10.06	9.70	9.78	10.72	10.91	11.27	8.48	8.39	8.17	10.38	9.46	8.28
Na_2O	2.08	2.62	2.35	1.87	2.25	2.40	2.88	2.50	3.62	3.88	4.07	3.32	2.96	3.47	3.36	3.54
K_2O	0.62	0.80	0.85	1.20	0.78	1.38	1.44	1.08	1.90	1.20	1.56	1.20	1.15	1.47	1.22	1.42
MnO	0.06	0.09	0.11	0.11	0.03	0.12	0.14	0.12	0.09	0.11	0.16	0.14	0.06	0.05	00.17	0.09
P_2O_5	0.16	0.12	0.05	0.18	0.12	0.15	0.11	0.17	0.14	0.21	0.30	0.19	0.16	0.12	0.18	0.15
H_2O	1.68	1.71	1.90	1.76	1.87	1.97	1.94	1.41	2.15	3.85	3.19	2.04	2.43	1.84	2.06	2.85
Total	100.00	100.01	99.98	100.02	100.12	100.05	100.04	99.99	100.00	100.07	99.98	100.00	100.01	100.00	100.19	99.99
SI	28.63	30.38	37.81	29.26	32.04	25.98	29.77	31.65	29.66	28.22	24.00	25.83	25.47	27.81	22.97	25.56
Al_2O_3/SiO_2	0.30	0.28	0.26	0.28	0.28	0.28	0.29	0.29	0.28	0.27	0.30	0.28	0.27	0.26	0.29	0.28
FeO^*/MgO	2.04	1.71	2.03	1.95	1.67	2.16	1.73	1.65	1.56	1.62	2.01	2.00	2.10	1.81	2.35	1.95
Fe_2O_3/FeO	0.24	0.25	0.21	0.24	0.23	0.22	0.19	0.19	0.15	0.10	0.12	0.16	0.21	0.17	0.13	0.14
NORM																
Q	1.26	0.48	3.48	5.34	3.54	2.04	-	-	-	-	-	1.50	5.46	-	-	0.66
Or	3.89	5.00	5.00	7.23	4.45	8.34	8.34	6.12	11.12	7.23	9.45	7.23	6.67	8.90	7.22	8.34
Ab	17.82	22.01	19.91	15.72	18.86	20.44	24.10	20.96	18.72	24.63	32.88	28.30	25.15	27.36	28.29	29.87
An	28.63	24.82	25.02	27.52	26.41	23.63	21.68	25.02	14.73	14.73	16.96	21.41	22.80	15.85	21.96	19.46
Ne	-	-	-	-	-	-	-	-	7.95	4.34	0.92	-	-	1.07	-	-
Di Wo	14.73	14.15	10.90	9.86	9.51	9.86	11.25	11.37	16.12	16.82	9.86	8.12	7.08	14.50	10.09	8.70
Di En	7.30	8.80	8.50	5.30	5.30	4.96	5.90	6.20	8.90	9.00	4.90	4.10	3.69	7.70	4.60	4.50
Di Fs	7.13	5.81	5.15	4.22	3.84	4.67	5.02	4.75	6.60	7.26	4.75	3.83	3.18	4.63	5.41	3.96
Hy En	6.30	6.10	8.90	9.70	11.40	8.70	2.02	5.08	-	-	-	8.90	8.70	-	5.30	8.10
Hy Fs	5.12	5.28	8.58	7.00	7.92	8.26	1.32	6.60	-	-	-	8.58	7.66	-	6.07	7.39
Ol Fo	-	-	-	-	-6	-	6.30	4.34	5.74	3.58	5.28	-	-	5.18	5.18	1.26
Ol Fa	-	-	-	-	-	-	6.12	1.43	4.69	2.96	5.71	-	-	4.49	1.63	-
Mt	3.02	3.02	3.02	3.02	3.01	3.25	2.78	2.55	1.86	1.16	1.62	2.09	2.55	2.32	1.85	1.86
Il	3.04	2.58	2.58	3.96	3.65	3.65	2.74	3.80	4.10	3.95	3.80	3.65	4.26	4.10	4.10	4.10
Ap	0.34	0.34	-	0.34	0.34	0.34	0.34	0.34	0.34	0.34	0.67	0.34	0.34	0.34	0.34	0.34

TABLE III - Continued

Chemical and normative composition of the Panjal Traps

Flow No.	17	18	19	20	21	22	23	24	25	26	27	28	29	30	31	32
SiO_2	47.56	55.38	54.78	47.97	49.97	51.13	53.95	52.43	51.00	48.20	55.52	55.52	50.77	50.12	52.32	48.79
TiO_2	2.04	1.64	1.54	1.71	1.52	2.01	1.58	1.56	1.35	1.44	1.64	1.42	1.48	1.54	1.43	1.36
Al_2O_3	14.58	13.53	14.70	14.09	12.55	14.15	15.15	14.61	15.24	14.60	13.40	17.14	13.57	14.21	15.85	14.23
Fe_2O_3	2.14	1.83	1.66	1.84	1.25	2.20	1.85	1.81	1.82	3.23	1.99	1.12	2.50	2.00	2.27	2.12
FeO	9.50	9.80	9.21	8.91	9.76	10.57	8.18	8.52	8.13	9.05	8.25	6.30	8.91	8.75	8.29	8.95
MgO	6.92	4.22	3.86	7.46	5.63	4.59	4.18	6.08	6.02	7.13	4.36	3.50	5.38	6.17	4.53	6.76
CaO	11.19	6.84	8.37	11.27	12.31	9.34	8.83	9.97	9.86	9.97	9.35	8.04	9.98	9.72	8.84	10.46
Na_2O	2.70	3.55	3.15	3.44	3.47	2.68	3.69	2.25	3.96	3.50	3.78	2.95	3.63	3.55	4.11	3.37
K_2O	0.95	1.13	0.76	1.05	1.37	1.20	0.59	0.76	0.68	1.15	1.18	1.69	1.45	1.51	0.72	1.07
MnO	0.08	0.09	0.11	0.15	0.14	0.17	0.15	0.16	0.17	0.16	0.11	0.07	0.14	0.15	0.09	0.15
P_2O_5	0.19	0.23	0.24	0.25	0.14	0.15	0.18	0.20	0.21	0.10	0.16	0.09	0.14	0.19	0.19	0.20
H_2O	2.16	1.71	1.72	1.88	1.92	1.86	1.77	1.83	1.57	1.67	1.80	2.21	2.17	2.14	1.49	2.54
Total	99.97	99.95	100.19	100.03	100.03	100.05	100.10	100.09	100.01	100.20	100.14	100.05	100.12	100.05	100.13	100.00
SI	31.16	20.53	20.71	33.35	26.14	22.62	22.61	31.44	29.21	30.20	22.36	22.49	24.93	28.53	22.74	30.37
Al_2O_3/SiO_2	0.31	0.24	0.27	0.30	0.25	0.27	0.28	0.28	0.30	0.30	0.25	0.31	0.26	0.29	0.29	0.29
FeO^*/MgO	1.68	2.75	2.82	1.44	1.96	2.78	2.40	1.70	1.65	1.72	2.35	2.12	2.12	1.74	2.33	1.64
Fe_2O_3/FeO	0.23	0.19	0.18	0.20	0.13	0.21	0.22	0.21	0.21	0.36	0.24	0.18	0.28	0.23	0.26	0.23
								NORM								
Q	-	7.02	8.04	-	-	2.64	4.50	5.76	-	-	2.58	8.16	-	-	-	-
Or	5.56	6.67	4.45	6.12	8.34	7.23	3.34	3.89	3.89	6.67	7.23	10.01	8.34	8.90	4.45	6.12
Ab	22.53	29.87	26.72	20.17	19.91	22.53	31.44	18.86	33.54	24.10	31.96	25.15	29.87	27.77	34.58	25.15
An	24.74	17.79	23.63	20.02	14.46	23.03	23.07	27.80	21.68	20.85	15.85	28.36	16.40	18.35	22.52	20.85
Ne	0.28	-	-	4.83	5.11	-	-	-	-	2.84	-	-	0.57	1.14	-	1.70
Di Wo	12.53	6.03	6.73	14.27	19.14	9.40	8.35	9.05	11.37	11.60	12.41	4.52	13.80	12.18	8.58	12.64
Di En	7.00	2.60	2.80	8.20	9.70	4.10	4.00	4.90	6.20	6.60	6.00	2.30	7.10	6.50	4.22	6.90
Di Fs	5.02	3.43	3.96	5.41	8.98	5.21	4.36	3.83	4.75	4.90	6.20	2.11	6.34	5.28	4.22	5.28
Hy En	-	7.90	6.80	-	-	7.40	6.40	10.30	0.30	-	4.90	6.40	-	-	4.70	-
Hy Fs	-	10.69	9.37	-	-	9.24	7.00	8.05	0.20	-	5.02	6.21	-	-	4.49	-
Ol Fo	7.28	-	-	7.26	3.08	-	-	-	5.88	7.84	-	-	4.35	6.30	1.68	7.00
Ol Fa	5.71	-	-	5.41	4.28	-	-	-	5.10	5.81	-	-	4.49	5.50	1.84	5.92
Mt	3.02	2.55	2.32	2.55	1.86	3.25	2.78	2.55	2.55	4.64	2.78	1.62	3.71	2.78	3.25	3.02
Il	3.80	3.04	2.89	3.19	2.89	3.80	2.74	2.89	2.58	2.74	3.04	2.74	2.74	2.89	2.74	2.58
Ap	0.34	0.67	0.67	0.67	0.34	0.34	0.34	0.34	0.34	0.34	0.34	0.34	0.34	0.34	0.34	0.34

$FeO^* = Fe_2O_3 + FeO$

generally have similar variation trends in unaltered volcanic series. If the analysis value of Fe_2O_3 is less than this (percent TiO_2 + 1.5), no correction is required; if the value is higher, the "excess" amount of Fe_2O_3 is converted to FeO.

This procedure causes changes in mafic mineral content by several percent in the normative composition, but has little effect on other parameters such as Iron/Magnesium ratio. The purpose of this adjustment is to obtain the composition as close as possible to the primary composition of the rock.

Table III shows the average chemical composition along with the normative composition and various oxide ratios of the 32 flows of the Panjal Traps. It is seen from this Table that the total alkali content of these rocks generally lies between 4 and 5 percent and the Fe_2O_3 value is generally around 2 percent. This does not strictly warrant post-extrusion correction for Fe_2O_3. Also, following Chayes (1966) the Panjal Traps need no post-extrusion Fe_2O_3 correction since Fe_2O_3/FeO ratio is far below 0.6. Similarly, according to Irvine and Baragar's (1971) equation, except for Flow No.26, all the other flows have Fe_2O_3 values within the recommended percentage set by the equation.

The influence of alkali metasomatism is clearly depicted by the normative analyses data (Table III). There is very

high percentage of albite and orthoclase in the norm which is due to very high Na_2O and K_2O in the rock. The possibility of the original alkali-rich character of the magma may be ruled out on the basis of the abundance of secondary albite and biotite in these rocks. Such rocks have proportionally high alkali content. Wherever secondary albite and biotite are less or absent in the rock, alkali content of that sample is low (normal for a silica saturated rock) and olivine or nepheline does not build up in the norm of that particular analysis. Such an inference is also supported by other parameters like MgO - Al_2O_3/SiO_2 , Fe_2O_3/FeO, et cetra, dealing with the silica-saturated versus silica-undersaturated nature of a particular magma.

Variation Diagrams

Murata (1960) devised a method utilizing various variation diagrams in which weight percent of MgO, CaO, or K_2O + Na O are plotted against Al_2O_3/SiO_2 weight ratio to determine the nature of the magma, whether tholeiitic or alkaline. MgO is strongly affected with the progressive fractionation of the basic magma towards acidic members and shows a downward trend. CaO behaves similarly whereas Na_2O and K_2O show reverse trend but in these cases, slopes of the trend lines are not as steep as it is for MgO. In the Panjal Traps alkali metasomatism has changed the original alkali content and as such use of total alkali was not preferred to decipher the nature

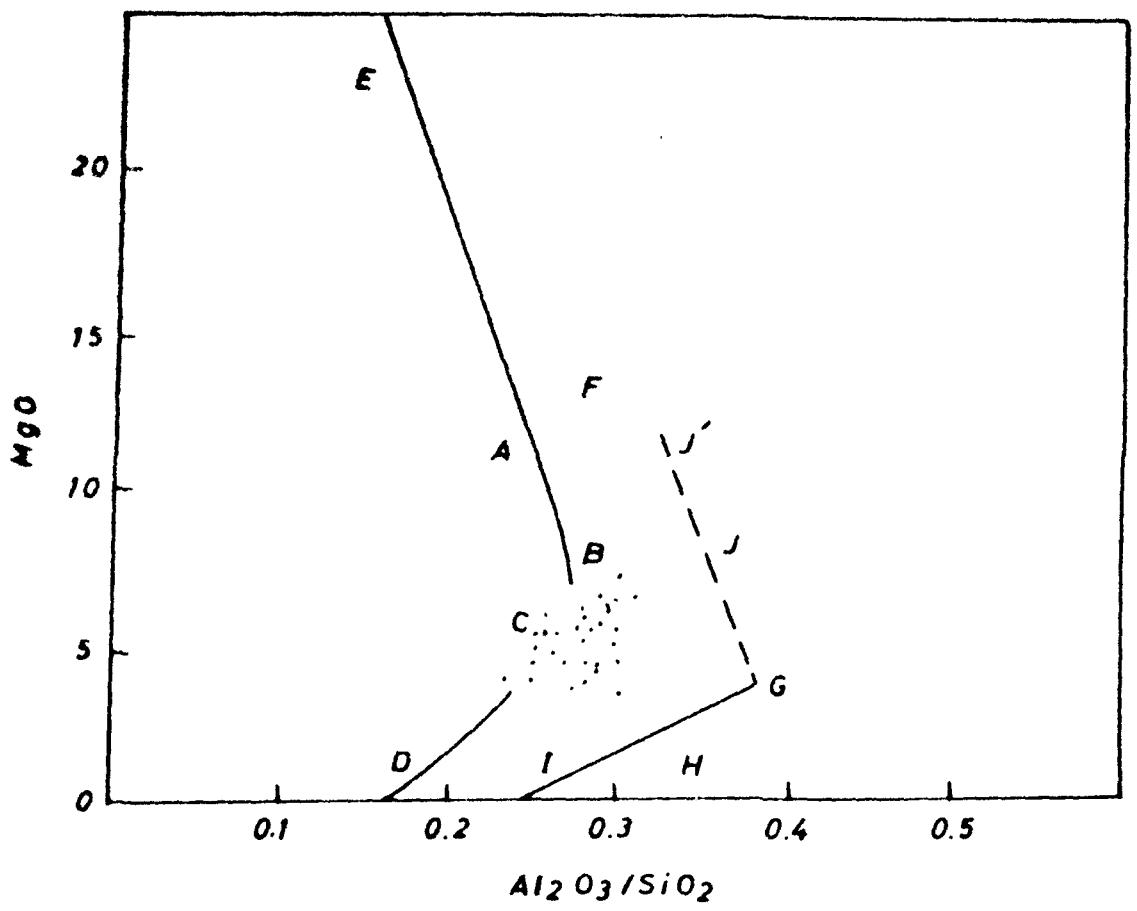

Figure 7. Plots of the Panjal Traps on $MgO - Al_2O_3/SiO_2$ (Murata, 1960) variation diagram

Tholeiitic basalt series

- A. Tholeiitic olivine basalt
- B Tholeiitic basalt
- C Quartz basalt
- D Granophyre
- E Picrite (oceanite)

Alkali basalt series

- F. Ankaramite
- G. Hawaiite (andesine andesite)
- H. Mugearite (oligoclase andesite)
- I. Trachyte
- J Alkalic basalt
- J'. Alkalic olivine basalt

of the magma. Instead, MgO versus Al_2O_3/SiO_3 variation diagram has been used (Figure 7). The points in this diagram fall on tholeiite trend line and cluster near the tholeiitic basalt (B) and quartz-basalt (C) fields, mainly in the region mid-way between the two. The less basic character, as indicated by the chemical analyses of these rocks, is also evident from these plots. Also, the points lie away from the more differentiated members (D) in the diagram. As the points do not extend beyond C (quartz-basalt), it may be inferred that the Panjal magma did not fractionate beyond quartz-basalt stage, and represent generally evolved, but still basaltic, composition. Such an inference is in conformity with the evolved nature of the plagioclase-pyroxene mineral assemblage of these rocks.

Another method to distinguish the nature of magma between tholeiite and alkali-olivine basalt is by using Fe_2O_3/FeO ratio. Kuno et al. (1957) found this ratio to be 0.5 and 0.3 for alkaline and tholeiitic rocks respectively. The higher value of this ratio for alkaline rocks is attributed to high partial oxygen pressure that attends the formation of these magmas at deeper levels in the mantle. The Fe_2O_3/FeO ratio of the Panjal Traps ranges between 0.10 to 0.38, which further suggests a tholeiitic descent. Lower values of Fe_2O_3/FeO ratio indicate low oxygen partial pressure during crystallization of the magma (Osborn, 1969), a feature that is attributed to low magmatic water content in the parental

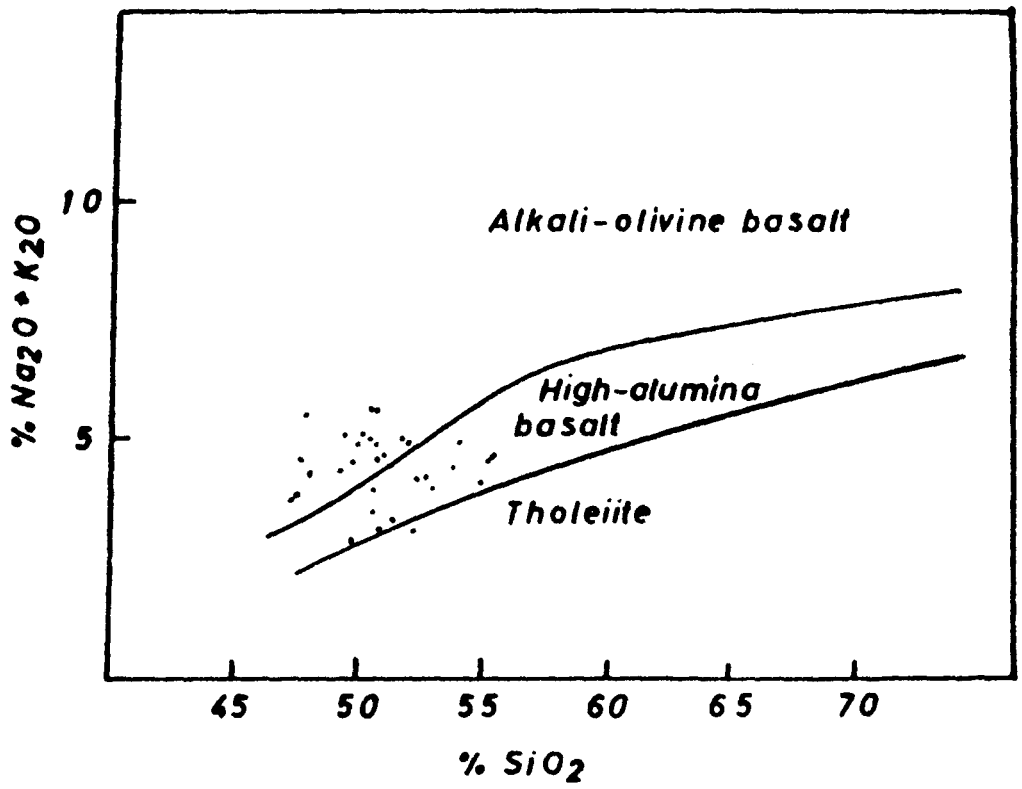

Figure 8. Alkali–silica diagram for the Panjal Traps. Subdivisions from Kuno (1968).

magma (Kuno, 1968). Absence of any primary hydrous mineral phase in the Panjal Traps also suggests that these magmas crystallized under low partial oxygen pressure. Water may have entered these rocks at a later stage after the solidification of magma and resulted in the formation of secondary hydrous minerals.

Kuno (1968) has shown that Cenozoic basalts of Japan, Korea, and Manchuria plot in three distinct regions on silica - total alkali diagram. The three types of basalts, viz.: tholeiite, high-alumina basalt, and alkali-olivine basalt, plot in three distinct regions. Figure 8 shows the plots of total alkali against silica for the Panjal Traps. The results are contrary to what has been inferred by earlier discussion since points for the Panjal Traps generally fall in the high-alumina and alkali-olivine basalt fields. It is evident from Figure 8 that the boundaries between the three basalt types at a particular silica value is primarily controlled by the amount of alkali content. With the increase in alkali content for a specific silica percentage, the plot will shift from tholeiite field to alkali-olivine basalt field through high-alumina basalt region. Considering the extent of alkali enrichment and the inference drawn from Figure 7, it is suggested that the Panjal Traps lying in the alkali-olivine basalt and high-alumina basalt fields may not represent the actual composition of the magma. Moreover, much low magnesium

content and absence of olivine in these rocks do not support the alkali-olivine basalt lineage of these rocks. Also, silica infilling in vesicles in these rocks indicates an oversaturated character of the magma (Holmes, 1964), as also indicated by the presence of normative quartz in those rocks which contain little or no secondary albite and biotite.

Irvine and Baragar (1971) found that more than half of the plots for Coppermine River lavas on silica a alkali diagram plot in alkali-olivine basalt field though these lavas are "certainly tholeiitic in their overall characteristics". Irvine and Baragar (op.cit.) concluded that such abnormal results indicate limitations of silica - alkali diagram. However, in Figure 8, the abnormal plots for the Panjal Traps may be attributed mainly to alkali enrichment in these rocks.

Figure 8 shows that the Panjal Traps from a coherent mass with little compositional variability. It may be suggested that the Panjal magma lies on a single line of descent or magmatic lineage, a coherence further suggested by the clustered nature of the points within a small region in all variation diagrams for these rocks.

On the basis of mineralogy and chemistry, Kuno (1950) distinguished tholeiitic basalt series from calc-alkaline series and designated them as "pigeonite series" and "hypersthene series" respectively. Pigeonite is the characteristic

groundmass pyroxene in tholeiite series whereas in calc-alkaline series, orthopyroxene, instead of pigeonite, is present in the groundmass. Although Miyashiro (1974) accepts the applicability of this classification in certain areas, he refutes the universality of this classification and, as an example of general inapplicability, reports the disagreement between mineralogy and chemistry in the Chakoi volcanic zone of Northeast Japan. Such disagreement has also been reported from areas outside Japan. Miyashiro (op.cit.) quotes the occurrence of hypersthene in the groundmass of some tholeiites in Hawaii as reported by Macdonald and Katsura (1964).

Miyashiro (op.cit.) proposed a chemical classification for calc-alkaline and tholeiite rock series. He defined a boundary line separating the two series that passes through two points (Fe_2O_3+ FeO/MgO = 0.5; SiO_2= 46%) and (Fe_2O_3+ FeO/MgO = 3.0; SiO_2 = 62%). This is represented by the following equation:

$$SiO_2(\text{percent}) = 6.4 \times Fe_2O_3 + FeO/MgO + 42.8$$

The tholeiite and calc-alkaline series are defined by gentler and steeper slope respectively than the division line. He also discussed other criteria for classification but found the above one "preferrable" when this division line is used, the "hypersthenic" rocks of the Chakoi volcanic zone of Northeast Japan, as defined by Kuno (1950), are found to plot both in

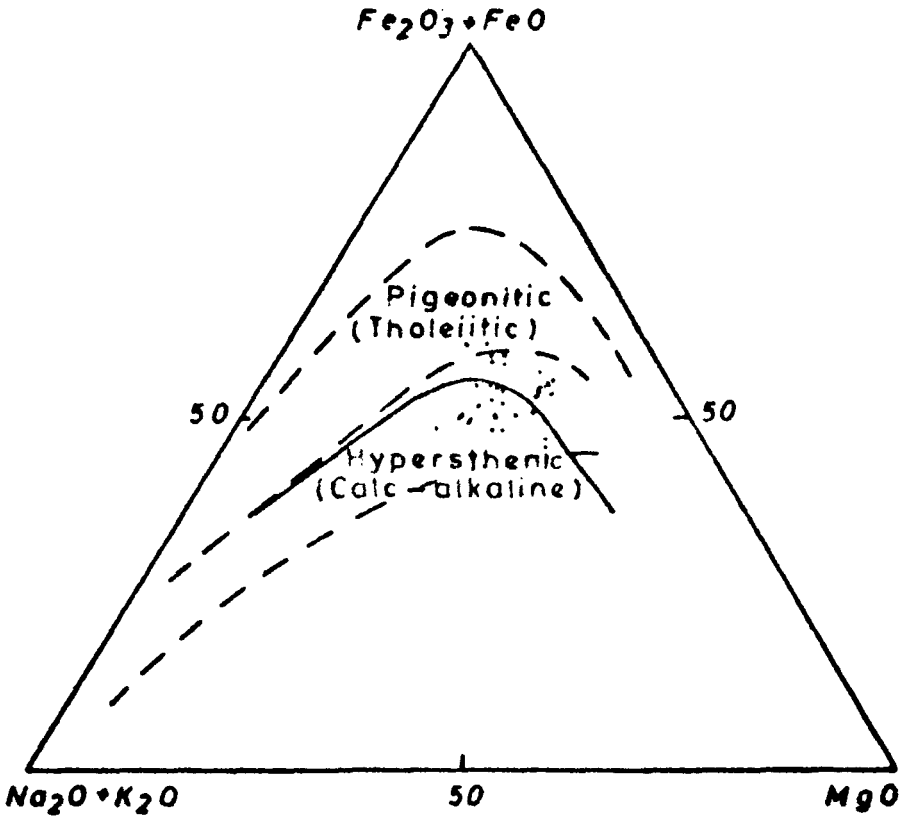

Figure. 9. MFA diagram for the Panjal Traps. Solid line represents the boundary between tholeiite and calc – alcaline rock series adopted from Irvine and Baragar (1971), and broken lines, from Kuno (1968), separate pigeonite and hypersthene rock series.

calc-alkaline and tholeiite fields on Miyashiro's (op.cit.) proposed diagram.

There is a general agreement that higher Fe_2O_3+ FeO, higher Fe_2O_3 + FeO/MgO ratio, and lower Mg x 100/MgO + Fe_2O_3 + Na_2O + K_2O (Solidification Index, SI) characterise tholeiite series. Kuno (1968) found that tholeiite series plot in a distinct region that is different from calc-alkaline series region on SiO_2 — SI and Fe_2O_3 + FeO — SI diagrams. Tholeiite series is devoid of any primary hydrous silicate mineral whereas in calc-alkaline series hydrous minerals, such as hornblende and biotite, are always present. Crystallization temperature of tholeiite series is higher than calc-alkaline series because the latter series form under higher water pressure conditions. Higher oxygen pressure in calc-alkaline series causes early separation of magnetite and thus explains lack of iron concentration during the fractionation of this series.

Figure 9 shows that majority of the plots for the Panjal Traps lie in calc-alkaline field on MFA diagram. This goes against the inferred tholeiitic character of these rocks. Kuno (1968), using his proposed division line between pigeonite (tholeiite) and hypersthene (calc-alkaline) rock series in MFA diagram, also found some of the plots for pigeonite rock series of Hatizyo-zima volcano of central Japan and tholeiitic rocks of Scottish Tertiary Province fall within

calc-alkaline field. Kuno (op.cit.) accounted for the discrepancy in the plots of Hatizyo-zima volcano by the presence of abundant plagioclase phenocrysts in these rocks. Though Kuno (op.cit.) does not define the nature of plagioclase phenocrysts in these rocks, presumably they are not much calcic. Plagioclase being a solid solution of Ca and Na, abundance of these crystals with relatively higher sodic composition will increase Na_2O content in the chemical composition of the rock. Since Na_2O alone, and not CaO, is used in the MFA diagram, an increased value of Na_2O will have an appreciable effect in causing a shift of plots towards the alkali end member and thus, into the hypersthenic region on this diagram, especially for rocks of early and middle stage fractionation. During the early stage of fractionation, the boundary line separating the two fields lies nearly parallel to Mg - Fe tie line, and the field of tholeiite series during this stage is narrow. A little increase in alkali content relative to MgO and FeO may cause the shift of the points into the calc-alkaline field from originally tholeiite field. Contrary to this, there is likely to be very little effect of alkali enrichment during late stage of fractionation as the boundary curve separating the two fields during this stage is almost parallel to the Alkali-Fe tie line.

However, when the discriminating boundary between calc-alkaline and tholeiite basalts as proposed by Irvine and

Baragar (1971) is employed, instead of the one suggested by Kuno (1968), the pigeonite rocks of Hatizyo-zima and the Scottish Tertiary Province completely plot in the tholeiite field. This may indicate the drawbacks of the Kuno's (1960) proposed discriminant boundary between pigeonite and hypersthene rocks. However, the Irvine and Baragar's (1971) division line also fails to bring out clearly the tholeiitic nature of the Copper Mine River lavas; most of the points for these rocks fall in calc-alkaline region. Miyashiro (1974) concluded that MFA diagram is not suitable for quantitative discussions on calc-alkaline and tholeiitic rock series.

The plots of the Panjal Traps that lie in calc-alkaline field in Figure 9 are largely governed by the high alkali content of these rocks rather than the limitations of the proposed discriminant boundary lines. Even if the analyses of the lower two porphyritic flows, containing abundant plagioclase phenocrysts, are excluded from the plots in Figure 9, most of the points still lie in the calc-alkaline series field. This does not support the view that abundance of plagioclase phenocrysts may shift the points from calc-alkaline to tholeiite field as suggested by Kuno (1968). In the Panjal Traps, the plagioclase phenocrysts may not have any effect on the plots of these rocks on MFA diagram because of the highly calcic composition of these crystals. However, if both Na_2O and K_2O are added, the proportion of the alkali in total MFA will be large and accordingly the shift of the plots will be more

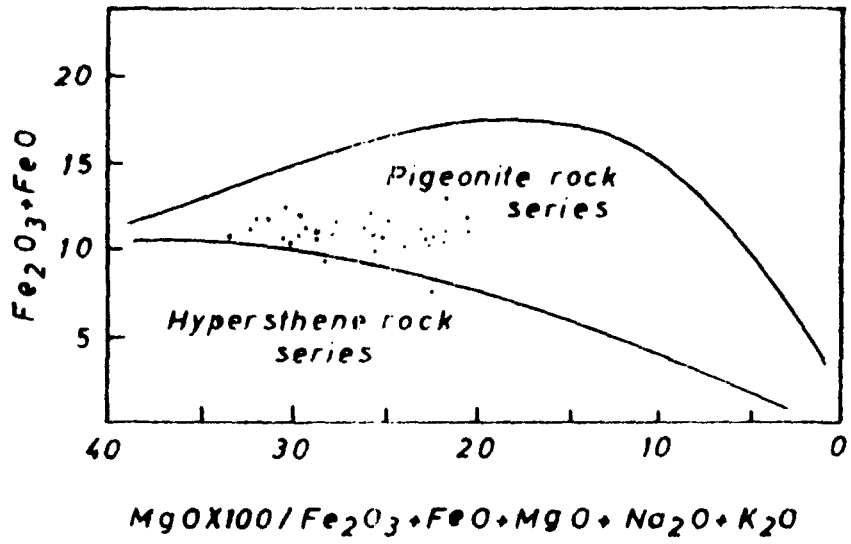

Figure 10. Total iron – SI diagram for the Panjal Traps. The boundary lines of the fields of pigeonitic and hypersthenic rock series from Kuno (1968).

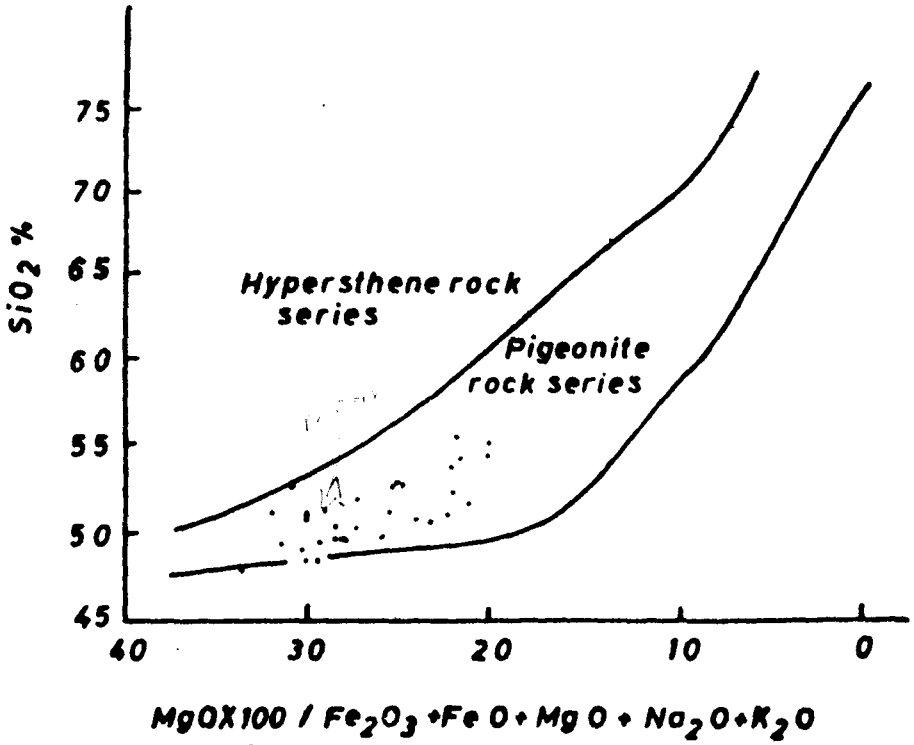

Figure 11 SiO_2 versus Si diagram for the Panjal Traps. Description of the boundary lines is the same as in Figure 10.

towards calc-alkaline field, particularly during the early stage of fractionation of these rocks. This seems to explain fairly well the picture depicted by the Panjal Traps in Figure 9. Alkali metasomatism appears to be responsible for their plots in calc-alkaline field. This fact is further supported by Figures 10 and 11 in which Fe_2O + FeO and SiO_2 respectively are plotted against SI. The Panjal Traps occupy tholeiite field on these diagrams; enrichment of alkali has insignificant effect on the fields of tholeiite and calc-alkaline basalts in these diagrams.

Typical tholeiitic nature of the Panjal Traps is also evident by the plots of SiO_2, Fe_2O_3 + FeO, and TiO_2 against Fe_2O_3 + FeO/MgO ratio as shown in Figure 12 a, b, and c.

Figure 13 shows all oxides plotted against Solidification Index (SI). The use of SI for the Panjal Traps, which represent early stage of fractionation of magma, has the advantage over the classical silica variation diagram, the former emphasises variation to a large extent in the early stage of fractionation (Kuno, 1957) whereas the latter fails to do so, instead, emphasises variation much more in the late stage of fractionation (Wager and Deer, 1939; Poldervaart, 1949). Solidication Index is the percentage of MgO in MFA diagram, It is accepted, in any fractionation trend plotted on MFA diagram, the composition of magma invariably changes thereby decreasing SI value. Kuno (1968) found close similarity

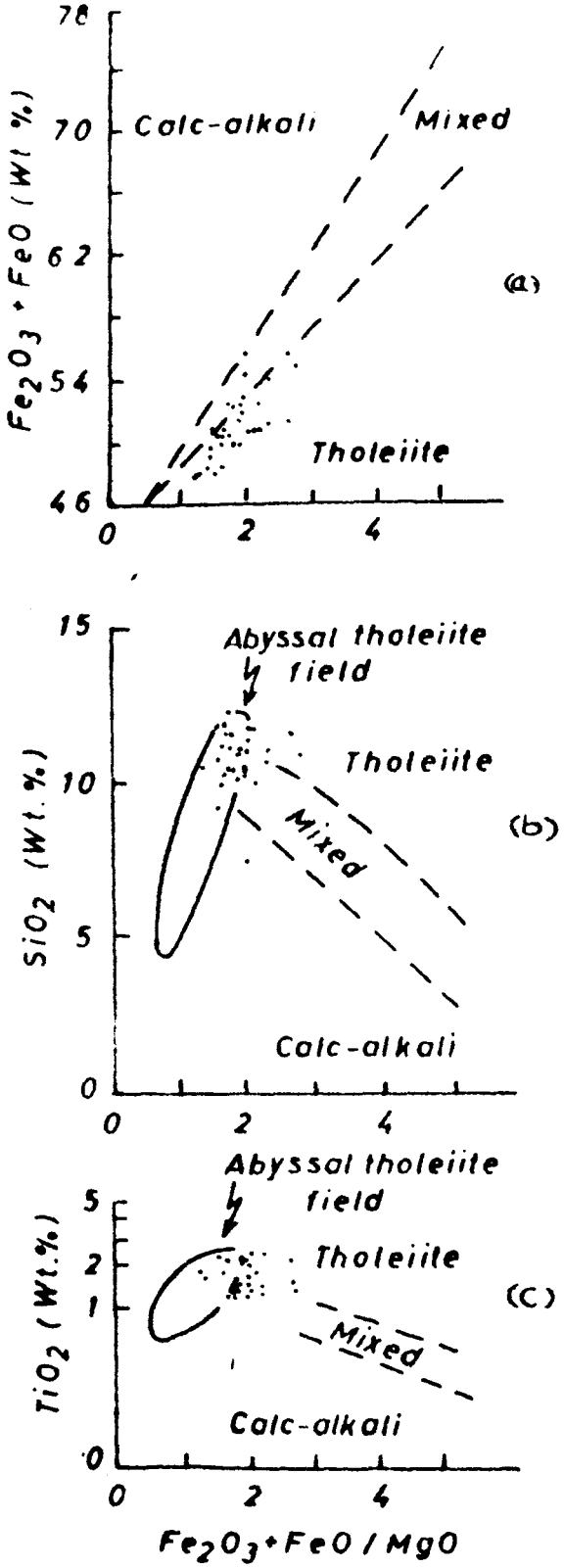

Figure 12. Plots of the Panjal Traps showing (a) SiO_2, (b) total iron, (c) TiO against Fe_2O_3 +FeO /MgO ratio boundary lines in the diagrams from Miyashiro and Shido (1975).

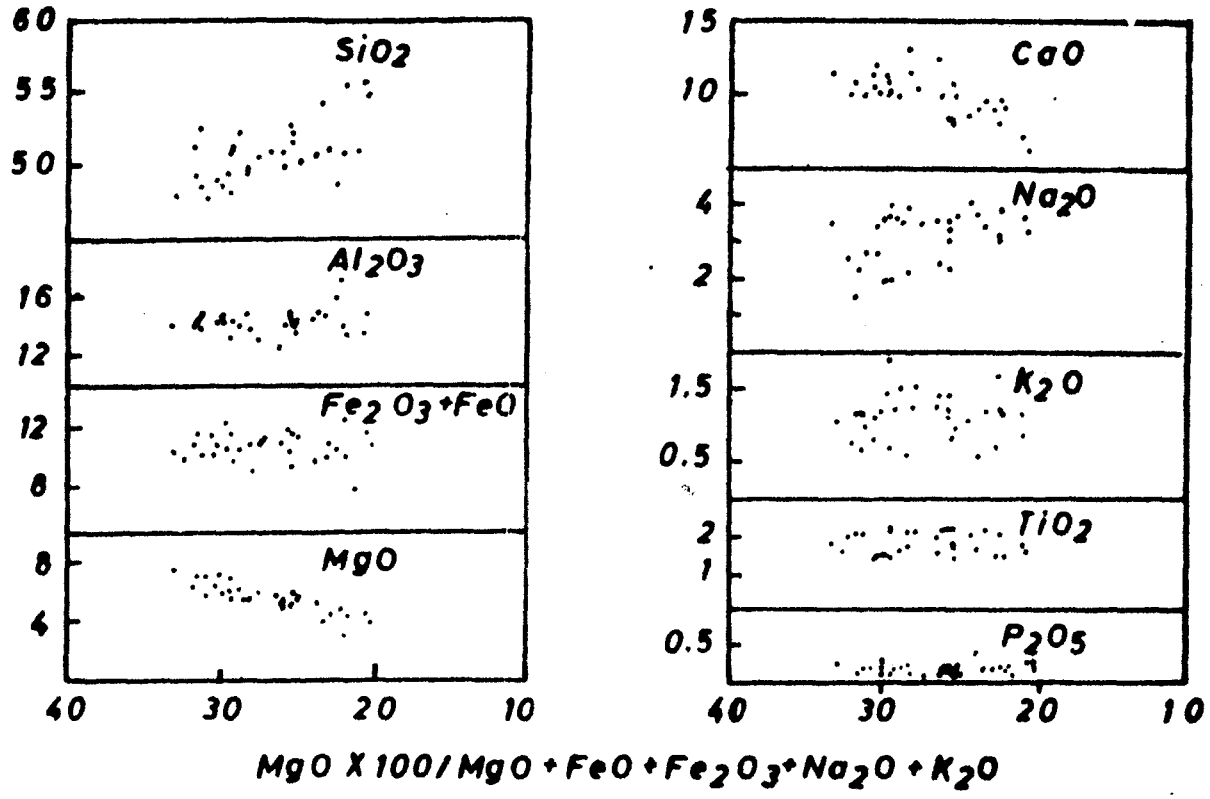

Figure 13. Solidification Index variation diagram for the Panjal Traps.

between his plots of various oxides against SI and those of Wager (1960) plotted against the percent solidified for successive liquids of Skaergaard. Kuno (1968) expressed doubt about the proportionality of SI with fractionation stage in other igneous series. In the Panjal Traps MgO shows a steep downward linear trend with the decrease in SI (Figure 13). As such use of SI, instead of SiO_2 , was preferred in Figure 13.

It may be expected that later enrichment of alkalis in the Panjal Traps may not give true values of SI for these rocks and, therefore, plots in Figure 13 may not depict the exact picture of variation of various oxides. In Figure 13, SI occupies ordinate based on MgO x 100/mgO + Fe_2O_3 + FeO + Na_2O + K_2O. The amount of alkalis in comparison with the total amount of the constituents of denominator is invariably less in basalts or basaltic andesites, as also in the Panjal Traps (Table III). Further, alkalis do not have any separate position or entity in SI as they have in MFA diagram where they form one end member. Hence, enrichment of alkalis will have very little effect on SI. For instance, on the basis of the average composition of the Panjal Traps (Table II) the SI value of the Panjal Traps is 27.01. When values for alkalis of the Karroo basalts (Table II), whose chemical composition, especially the percentage of total iron and magnesium, is closely similar to that of the Panjal Traps, are substituted for the values of alkalis in the Panjal Traps, the SI value

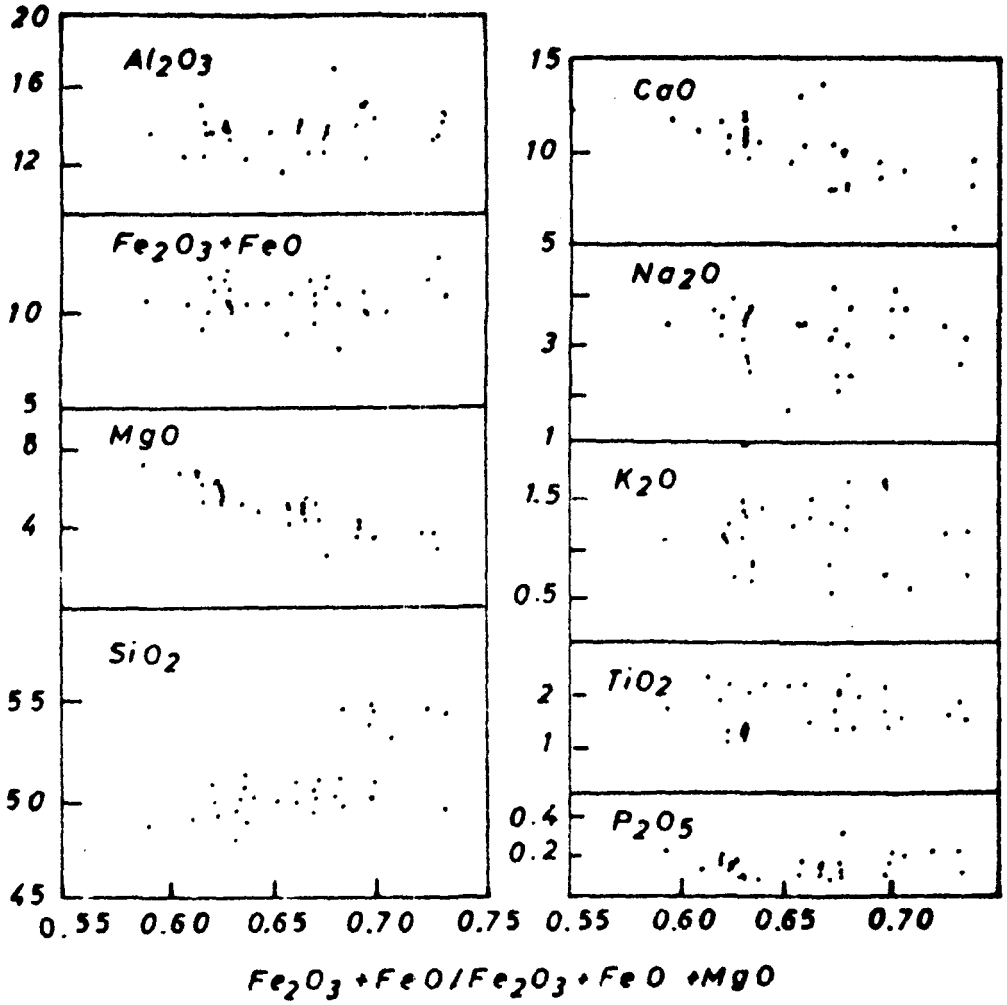

Figure 14. All major oxides of the Panjal Trap against $Fe_2O_3 + FeO / Fe_2O_3 + FeO + MgO$

comes to 27.31. Thus, such a small difference in SI may cause very little lateral displacement of the plots on oxide versus SI diagram towards lower SI leaving the trend of the plots unaffected.

It is evident from Table III that there is no apparent systematic variation in the major oxide chemistry of the Panjal Traps. However, many features concerning the chemistry and the changes therein with fractionation of the Panjal magma are exhibited in Figure 13. SiO_2 shows a slow rise with decreasing SI; total iron spreads widely for a given SI. Al_2O_3 do not show any particular trend. MgO shows a distinct and steep decrease with decrease in SI; CaO behaves similarly but the trend is not so distinct. Na_2O and K_2O show large spatter which supports the inference that alkali metasomatism has been random. Similar trends of various oxides are exhibited by the Panjal Traps when plotted against total iron/total iron + MgO (Figure 14).

Even with enriched alkali contents, the SI of the Panjal Traps ranges from 33 to 20.5 (Table III) which, when considered in their tholeiitic nature, indicates that these rocks are basalts and basaltic andesites. As most of the rocks have SI in the range of 29 to 20, basaltic andesites are inferred to be most abundant rock type.